

Geophysical Research Letters

RESEARCH LETTER

10.1029/2019GL082026

Key Points:

- The observations by the formation flight of Swarm satellites provide information on the spatial structure of plasma blobs
- Blobs are aligned in the northwest-southeast and southwest-northeast directions in the Northern and Southern Hemispheres
- The conjugate property and alignment support the association of those blobs with medium-scale traveling ionospheric disturbances

Correspondence to:

H. Kil,
hyosub.kil@jhuapl.edu

Citation:

Kil, H., Paxton, L. J., Jee, G., & Nikoukar, R. (2019). Plasma blobs associated with medium-scale traveling ionospheric disturbances. *Geophysical Research Letters*, 46, 3575–3581. <https://doi.org/10.1029/2019GL082026>




Received 11 JAN 2019

Accepted 17 MAR 2019

Accepted article online 20 MAR 2019

Published online 2 APR 2019

Plasma Blobs Associated With Medium-Scale Traveling Ionospheric Disturbances

Hyosub Kil¹ , Larry J. Paxton¹ , Geonhwa Jee² , and Romina Nikoukar¹ 

¹The Johns Hopkins University Applied Physics Laboratory, Laurel, MD, USA, ²Korea Polar Research Institute, Incheon, South Korea

Abstract Plasma blobs represent plasma density enhancements with respect to ambient plasma. The formation of blobs in low and middle latitudes is understood in association with either equatorial plasma bubbles or medium-scale traveling ionospheric disturbances (MSTIDs). This study reports four blob events identified from the Swarm satellite observations in 2014. Those blobs show the conjugate property and the alignment in the northwest-southeast direction in the Northern Hemisphere and southwest-northeast direction in the Southern Hemisphere. These are the typical characteristics of nighttime MSTIDs. The observation of MSTIDs in the total electron content maps and the absence of bubbles in the equatorial region at the times of the blob detection further support the association of those blobs with MSTIDs.

Plain Language Summary Three distinguishing mesoscale irregularity structures of the electron density in the low and middle latitude ionosphere are plasma bubbles, plasma blobs, and medium-scale traveling ionospheric disturbances (MSTIDs). Bubbles and blobs are plasma density depletions and enhancements, respectively, with respect to ambient plasma. MSTIDs are a wave-like modulation of the plasma density. Bubbles and MSTIDs are independent phenomena created by different mechanisms, but the formation of blobs is understood in association with either bubbles or MSTIDs. Our study reports blobs identified from Swarm satellite observations that show some of the characteristics of MSTIDs.

1. Introduction

Two notable mesoscale ionospheric structures in low and middle latitudes are bubbles and medium-scale (or mesoscale) traveling ionospheric disturbances (MSTIDs). Bubbles appear as plasma depletions relative to ambient plasma in the equatorial region and have elongated structures in the north-south direction. MSTIDs are a wave-like modulation of the plasma density and are often observed in middle latitudes. Another mesoscale ionospheric structure in low and middle latitudes is plasma blobs, which represent the plasma density enhancements relative to ambient plasma. Bubbles and MSTIDs are understood as independent phenomena because they develop by different physical processes and occur at different latitudes. However, blobs are considered in association with either bubbles or MSTIDs. The origin of blobs has been questioned because blobs do not show the characteristics of known phenomena. Blobs sometimes occur with other density fluctuations and can be understood as a part of a wavelike structure. However, this observation does not provide useful information about the origin of blobs because a wave characteristic exists in other ionospheric phenomena including bubbles and MSTIDs. Moreover, the amplitude of a blob is distinguished from the amplitudes of the density fluctuations around the blob.

The idea of the bubble-blob connection is based on the observations of bubbles and blobs at the same magnetic meridian (Huang et al., 2014; Le et al., 2003; Martinis et al., 2009; Park et al., 2003; Yokoyama et al., 2007) and a certain level of similarity in the distributions of bubbles and blobs (Huang et al., 2014; Park et al., 2008). Numerical simulations have also shown the formation of blobs when bubbles develop (Krall, Huba, Joyce, et al., 2010; Krall, Huba, Ossakow, et al., 2010). However, the detection of blobs in the absence of bubbles indicates that bubbles are not a prerequisite for the development of blobs (Kil, Choi, et al., 2011, 2015). The idea of the MSTID-blob connection is supported by the observations of blobs at the locations of MSTIDs (Kil & Paxton, 2017; Miller et al., 2014) and some similarities in the occurrence climatology of blobs and MSTIDs (Choi et al., 2012; Haaser et al., 2012).

So far, the causal linkage of blobs with bubbles or MSTIDs is asserted by their coincident occurrence at the same magnetic meridian. However, the coincident observation of two phenomena (“blob and bubble” or

“blob and MSTID”) does not corroborate their connection; we need knowledge of the occurrence of both bubbles and MSTIDs because they can occur simultaneously. The observations by the formation flight of Swarm satellites provide information on the spatial structure of blobs. Our study uses this information for the assessment of the source of blobs. The total electron content (TEC) perturbation maps over Japan are used to support the interpretation of Swarm observations.

We report four blob events identified from the Swarm observations in 2014. The Swarm mission is described in section 2. In section 3, we present the observations of Swarm and TEC perturbation maps. The conditions required for the formation of blobs are discussed in section 4. Conclusions are given in section 5.

2. Description of Swarm Mission

Swarm is the European Space Agency's mission designed for high-precision and high-resolution measurements of the Earth's magnetic field. The Swarm mission consists of three satellites: Swarm-Alpha (Swarm-A), Swarm-Bravo (Swarm-B), and Swarm-Charlie (Swarm-C). Swarm satellites were launched on 22 November 2013 into near circular polar orbits. Swarm-A and Swarm-C are flying side by side, maintaining a longitudinal distance of about 1.5° at an altitude of ~ 470 km with an orbital inclination of 87.5° . Swarm-B is a stand-alone satellite with a slightly different orbit (altitude: ~ 520 km, inclination: 88°). The payloads of each satellite are a vector field magnetometer, an absolute scalar magnetometer, an electric field instrument, an accelerometer, and laser range reflector. The electric field instrument consists of a Langmuir Probe (LP) and thermal ion imager. Our study uses the measurements of the electron density by LP. The data sampling cadence of LP is 0.5 s.

3. Observational Results

We have manually looked for blobs orbit by orbit by examining the Swarm observations in 2014. Some blobs occur simultaneously with bubbles at the same magnetic meridian, and some blobs occur in the absence of bubbles. Here we present four blob detections that we can specify their sources based on their spatial structures. Two events were detected by two satellites near Japan, and two other events were detected by three satellites near 160°E and 285°E longitudes.

Figure 1a shows the measurements of the electron density by Swarm-A and Swarm-C on 11 February 2014. Swarm orbits are shown in Figure 1b. The locations of blobs are indicated by horizontal black bars in the density plots and vertical black bars in Swarm orbit plots. In Figure 1a, the locations of blobs are symmetric with respect to the magnetic equator. Note the alignment direction of the blobs in Figure 1b. By connecting blobs A and C in the Northern Hemisphere we can identify their alignment in the northwest-southeast direction. Blobs B and D in the Southern Hemisphere are aligned in the southwest-northeast direction. These alignments along with the conjugate property are the typical characteristics of nighttime MSTIDs (Martinis et al., 2011; Otsuka et al., 2004; Saito et al., 2001). The Swarm observations do not show the instantaneous blob structure because the Swarm-C spacecraft is ahead of the Swarm-A spacecraft by about 25 min. MSTIDs at night propagate toward the southwest in the Northern Hemisphere and toward northwest in the Southern Hemisphere (Otsuka et al., 2004). If we interpret those blobs in terms of MSTIDs and consider the propagation direction of MSTIDs, blobs C and D were located further north and south, respectively, from their current locations at the times of the blobs A and B detection. The TEC perturbation maps, produced by subtracting the 1-hr running average, are shown for 22:20 and 22:50 UT in Figure 1c. Wave-like TEC modulations are not obvious in the TEC perturbation maps. However, we can trace the southwestward movement of the TEC enhancement (black circle) with time by comparing the two maps. If the TEC enhancement extends to the northwest direction following the typical MSTID alignment, this matches the locations of blobs A and C. Because the absolute TEC value is about 20 total electron content unit (TECU) ($10^{16}/\text{m}^2$) at the location of the black circle, the TEC enhancement of 0.3 TECU corresponds to 1.5% increase in TEC. In satellite observations, the plasma density at the blobs is greater than that of the ambient by 40–60%. Thus, blobs are pronounced features in satellite observations, but they are not in TEC maps.

We can identify the simultaneous occurrence of blobs and bubbles at the same magnetic meridian using Swarm observations. Swarm orbits are nearly parallel to the magnetic meridian in the Asian sector. Irregularities or bubbles are absent in the equatorial region in Figure 1a, and therefore, we interpret that those blobs have no connection with bubbles. One may argue that the Swarm observations do not provide

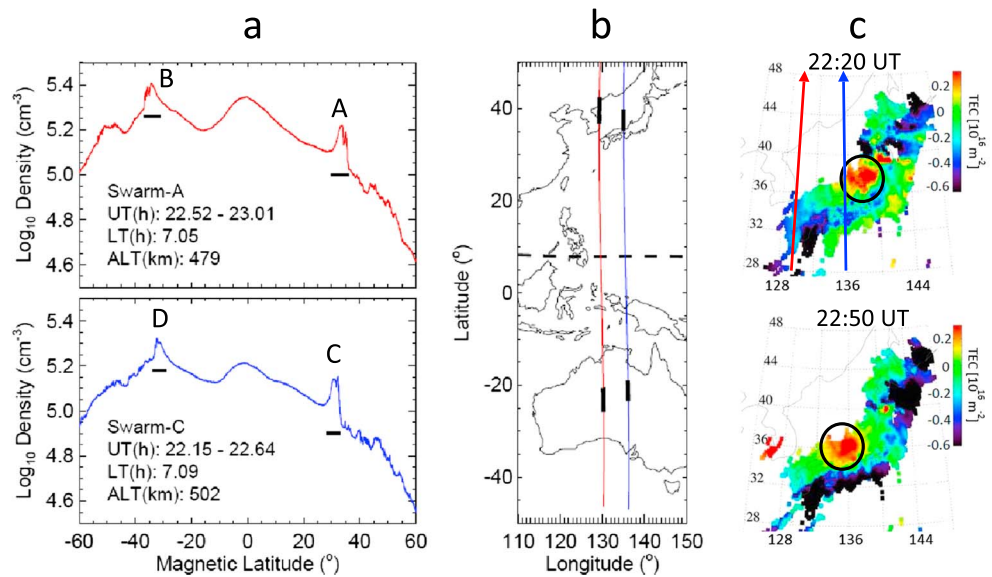


Figure 1. (a) Swarm-A and Swarm-C observations of the electron density on 11 February 2014. The observations were made around 7.0 hr LT. The locations of blobs are indicated by black horizontal bars. (b) Swarm-A (red) and Swarm-C (blue) orbits with the detection locations of blobs (black lines). The black dashed line indicates the magnetic equator. (c) Total electron content perturbation maps at 22:20 and 22:50 UT with Swarm-A and Swarm-C orbits by red and blue arrows, respectively. Black circles indicate the total electron content enhancements that might be related to blobs A and C.

accurate knowledge about bubbles at night because the observations were made at the time (7.0 hr LT) when the majority of bubbles decay away. However, we have identified the absence of bubbles in that longitude region on that night from the Communication/Navigation Outage Forecast System satellite observations.

Figure 2 is the same format as Figure 1 for the Swarm observations on 3 May 2014. The Swarm-A observations near the longitudes of Japan on 2 May 2014 are shown with black curves in Figure 2a. If we consider the structure of the background ionosphere being represented by black curves, then the features A–D are clearly perturbations. Those blobs are detected near midnight at ± 20 – 25° magnetic latitudes. The alignments of the pairs of blobs in Figure 2b are in the northwest-southeast direction in the Northern Hemisphere (blobs A and C) and in the southwest-northeast direction (blobs B and D) in the Southern Hemisphere. Because the time difference of the two Swarm satellites is only 6 min, the alignments are close to the instantaneous structure of the blobs. The TEC perturbation maps in Figure 2c show the development of wave-like structures at the locations of blobs. The wave structures have the typical characteristics of MSTIDs in the Northern Hemisphere; they are aligned to the northwest-southeast direction and propagate to the southeast direction. Bubble signatures do not appear in the equatorial region in Swarm observations (Figure 2a). Communication/Navigation Outage Forecast System data do not show bubbles in that longitude region either for this day and time.

Occasionally, three Swarm satellites fly side by side and provides information on the blob structure over a broader range. Figure 3 shows the Swarm observations and orbits on (a) 11 February 2014 and (b) 2 September 2014. Blobs are detected near midnight on both nights. The alignments of blobs on both nights are consistent with those observed near Japan in Figures 1 and 2. The time difference of the three orbits on 11 February 2014 is less than 20 min. On 2 September 2014, the Swarm-B observation was made about an hour after the Swarm-A and Swarm-C observations. If we assume that the blobs are associated with MSTIDs and the MSTIDs propagate toward southwest with a typical velocity of 50–100 m/s (Shiokawa et al., 2003), the location of the blob detected by Swarm-B is about 2 – 3° north from its current location at the time of the blob detection by Swarm-A and Swarm-C. After this adjustment the three blobs are nicely aligned in the northwest-southeast direction. Although we cannot identify the development of MSTIDs in those regions using TEC maps, the blob structure and the absence of bubbles in the equatorial region indicate that MSTIDs are the plausible sources of those blobs. In Figure 3b, the development of blobs is not as obvious in the Southern Hemisphere. Density fluctuations instead of blobs appear at the conjugate locations of the

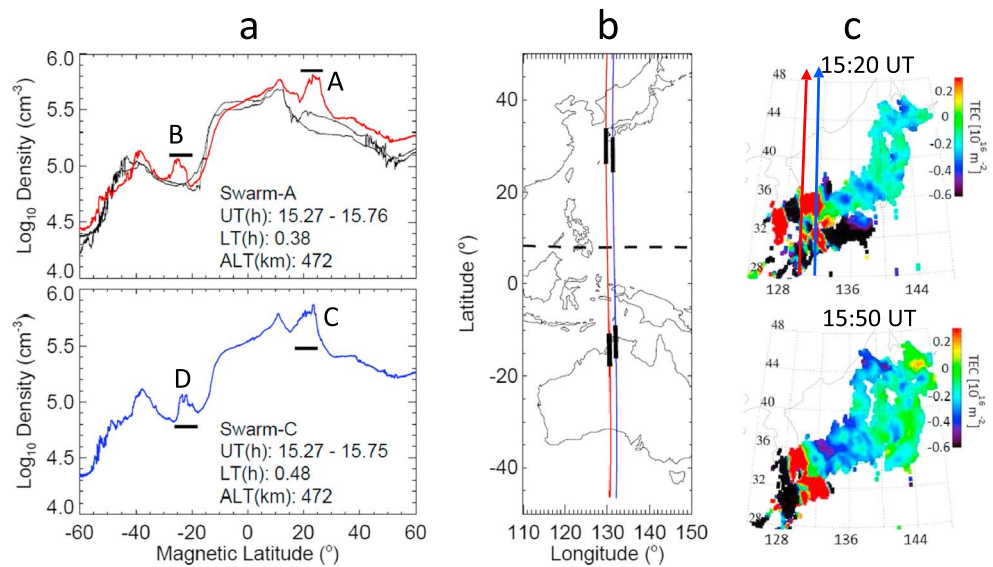


Figure 2. (a) Swarm-A and Swarm-C observations of the electron density on 3 May 2014. The observations were made just after midnight. The Swarm-A observations near the longitudes of Japan on 2 May 2014 are shown with black curves to infer the background structure of the ionosphere in the region. The locations of blobs are indicated by black horizontal bars. (b) Swarm-A (red) and Swarm-C (blue) orbits with the detection locations of blobs (black lines). (c) Total electron content perturbation map at 15:20 and 15:50 UT with Swarm-A and Swarm-C orbits.

blobs in the Northern Hemisphere. We have identified several blob events that are pronounced only in one hemisphere. This phenomenon can be understood by either the absence of conjugacy or the modification of blob structures by local ionosphere/thermosphere conditions. We do not yet have sufficient knowledge on how often blobs show the conjugate property.

4. Discussion

The spatial structure of the blobs that we report provides strong evidence of the association of blobs with MSTIDs. The MSTID signatures in the TEC perturbation maps at the locations of the blobs and the absence

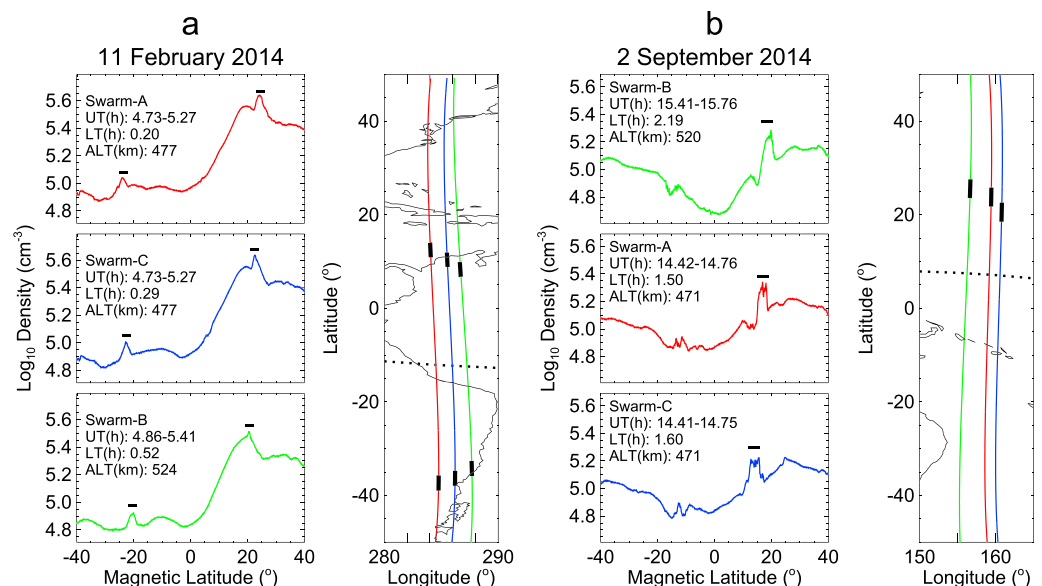


Figure 3. Swarm-A, Swarm-C, and Swarm-B observations of the electron density and their orbits (a) on 11 February 2014 and (b) on 2 September 2014 and their orbits. The locations of blobs are indicated by black bars.

of bubbles at the times of the blob detection further support the association of those blobs with MSTIDs. The conditions for the development of blobs from MSTIDs are an interesting science question, but this topic is out of the scope of our study; numerical simulations of MSTIDs under various ionospheric and thermospheric conditions are necessary to address this question. Here our discussion focuses on the physical processes in the ionosphere and thermosphere required for the explanation of blobs.

The variation of the plasma density at night in the low and middle latitude ionosphere is closely related to the changes in neutral composition and ionospheric height. The effect of neutral composition on the plasma density is pronounced in high and middle latitudes during geomagnetic storms (e.g., Crowley et al., 2006; Kil, Kwak, et al., 2011; Prölss, 1995). In general, the effect of the neutral composition change on the ionosphere results in the plasma density reduction in the *F* region. The expansion of the atmosphere by the heating of the atmosphere (a decrease in the ratio of atomic oxygen number density to molecular nitrogen number density [O/N_2 ratio]) increases the plasma loss rate by enhancing the loss path through the dissociative recombination of oxygen ions. The opposite phenomenon (plasma density enhancement by the reduction of molecular gasses in the *F* region or an increase in the O/N_2 ratio) can occur in the region where neutral winds converge. However, a significant plasma density enhancement by the neutral composition change, especially during nonstorm periods, has not yet been reported. If the change in neutral composition played a significant role in the formation of blobs, the TEC enhancement would also be significant at the locations of blobs. However, the TEC enhancement at the locations of blobs was less than 2% supporting the idea that a blob is not a plasma density enhancement in the total column.

Uplift of the *F* region peak is a more realistic formation mechanism for blobs. We note that the uplift cannot be so severe as to move the *F* peak height above the satellite altitude. Otherwise, a plasma depletion (or bubble) instead of a blob would appear in satellite observations. The *F* region can be lifted along magnetic field lines by neutral drag or perpendicular to the field lines (i.e., $\mathbf{E} \times \mathbf{B}$ drift) by an electric field. The upward plasma motion at the locations of blobs with respect to the background ionosphere is identified from satellite observations (Le et al., 2003; Park et al., 2003). We do not have ionosphere/thermosphere observation data for the assessment of the contributions of the two effects, but the conjugate property in blobs and the alignment of blobs into a specific direction in both hemispheres indicate the involvement of electric fields in the formation of blobs. The neutral drag, which is effective locally, may cause the hemispheric asymmetry in the blob intensity. In the Northern Hemisphere, the alignment of MSTID phase fronts in the northwest-southeast direction produces a plasma density inhomogeneity in the direction perpendicular to the alignment. Winds (\mathbf{U}) induce the Pedersen current in the $\mathbf{U} \times \mathbf{B}$ direction, and polarization electric fields develop due to the inhomogeneity in the Pedersen current (Makela & Otsuka, 2011; Otsuka et al., 2009). Blobs can arise from the eastward components of the polarization electric fields in the low density or high density region depending on the wind direction (e.g., Kil, Choi, et al., 2011).

We estimate the magnitude of the required uplift for the explanation of the observed blobs using a model ionosphere. Figure 4a shows the profiles of the electron (black dashed line), oxygen ion (blue), and hydrogen ion (red) densities at 15.5 hr UT (0.17 hr LT) on 3 May 2014 at 130°E longitude and 30°N latitude obtained from the International Ionosphere Reference model. The model data are chosen to compare with the blobs in Figure 2. The percentage changes of the electron density at the altitudes of 500 km (black), 600 km (blue), 700 km (green), and 800 km (red) by the simple uplift of the whole ionosphere are shown in Figure 4b. The percentage increase of the density is greater at the lower part of the topside *F* region. At an altitude of 500 km, the uplift of the ionosphere by 50 km causes about 50% increase in the density. The changes of the oxygen ion and hydrogen ion densities at an altitude of 500 km are shown in Figure 4c as a function of the magnitude of the uplift. As expected, the uplift produces the anticorrelation between the oxygen and hydrogen ion densities. This anticorrelation at the locations of blobs is identified by observations (Kil, Choi, et al., 2011). The detection of blobs in Figures 1–3 can be explained by the uplift of the ionosphere by 20–70 km. Assuming an effective vertical velocity of 50 m/s, the ionosphere is lifted up to 50 km in 1,000 s (16.7 min).

The ionospheric changes associated with the uplift will be much more complex than our simple calculations described above. TEC does not change in our calculation because the whole *F* region is simply moved vertically. However, the uplift of the ionosphere accompanies the plasma redistribution along magnetic field

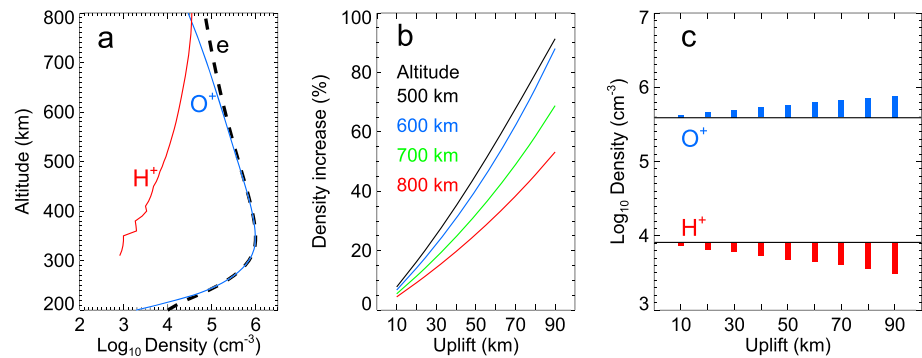


Figure 4. (a) Profiles of the total electron density (black dashed line), hydrogen ion density (red), and oxygen ion density (blue) derived from the International Ionosphere Reference model. The model data were obtained at 15.5 hr UT (0.17 hr LT) on 3 May 2014 at 130°E longitude and 30°N latitude. (b) Percentage increase of the total electron density at constant altitudes as a function of the *F* region uplift. (c) The dependence of the oxygen ion and hydrogen ion densities on the uplift at an altitude of 500 km.

lines and the plasma density enhancement in the total column by the reduction of the loss rate of the oxygen ion. These processes can affect the TEC at the location of a blob.

5. Conclusions

The formation flight of Swarm satellites provides a unique opportunity to identify the horizontal structure of blobs. From a preliminary survey of Swarm observations at low and middle latitudes in 2014, we have identified blobs that show the conjugate property and the alignment in the northwest-southeast direction in the Northern Hemisphere and in the southeast-northwest direction in the Southern Hemisphere. These are the characteristics of nighttime MSTIDs. The detection of MSTIDs by TEC perturbation maps near the locations of the blobs and the absence of bubbles in the equatorial region at the times of the blob detection further support the association of those blobs with MSTIDs. However, we do not know yet to what extent the creation of blobs can be attributed to MSTIDs and under what conditions blobs develop from MSTIDs. Statistical analysis of the characteristics of blobs and numerical simulations of MSTIDs under various ionosphere/thermosphere conditions are necessary to address these questions.

Acknowledgments

The work at JHU/APL was supported by MURI FA9559-16-1-0364 and KOPRI PE18020 awards. The authors acknowledge the Swarm team for the Swarm data. Swarm data and GPS TEC perturbation images are available in the websites <https://earth.esa.int/web/guest/missions/esa-operational-eo-missions/swarm> and <http://seg-web.nict.go.jp/GPS/GEONET/MAP>, respectively.

References

- Choi, H.-S., Kil, H., Kwak, Y.-S., Park, Y.-D., & Cho, K.-S. (2012). Comparison of the bubble and blob distributions during the solar minimum. *Journal of Geophysical Research*, *117*, A04314. <https://doi.org/10.1029/2011JA017292>
- Crowley, G., Hackert, C. L., Meier, R. R., Strickland, D. J., Paxton, L. J., Pi, X., et al. (2006). Global thermosphere-ionosphere response to onset of 20 November 2003 magnetic storm. *Journal of Geophysical Research*, *111*, A10S18. <https://doi.org/10.1029/2005JA011518>
- Haaser, R. A., Earle, G. D., Heelis, R. A., Klenzing, J., Stoneback, R., Coley, W. R., & Burrell, A. G. (2012). Characteristics of low-latitude ionospheric depletions and enhancements during solar minimum. *Journal of Geophysical Research*, *117*, A10305. <https://doi.org/10.1029/2012JA017814>
- Huang, C.-S., Le, G., de La Beaujardiere, O., Roddy, P. A., Hunton, D. E., Pfaff, R. F., & Hairston, M. R. (2014). Relationship between plasma bubbles and density enhancements: Observations and interpretation. *Journal of Geophysical Research: Space Physics*, *119*, 1325–1336. <https://doi.org/10.1002/2013JA019579>
- Kil, H., Choi, H.-S., Heelis, R. A., Paxton, L. J., Coley, W. R., & Miller, E. S. (2011). Onset conditions of bubbles and blobs: A case study on 2 March 2009. *Geophysical Research Letters*, *38*, L06101. <https://doi.org/10.1029/2011GL046885>
- Kil, H., Kwak, Y.-S., Lee, W. K., Miller, E. S., Oh, S.-J., & Choi, H.-S. (2015). The causal relationship between plasma bubbles and blobs in the low-latitude *F* region. *Journal of Geophysical Research: Space Physics*, *120*, 3961–3969. <https://doi.org/10.1002/2014JA020847>
- Kil, H., Kwak, Y.-S., Paxton, L. J., Meier, R. R., & Zhang, Y. (2011). O and N₂ disturbances in the *F* region during the 20 November 2003 storm seen from TIMED/GUVI. *Journal of Geophysical Research*, *116*, A02314. <https://doi.org/10.1029/2010JA016227>
- Kil, H., & Paxton, L. J. (2017). Global distribution of nighttime medium-scale traveling ionospheric disturbances seen by Swarm satellites. *Geophysical Research Letters*, *44*, 9176–9182. <https://doi.org/10.1002/2017GL074750>
- Krall, J., Huba, J. D., Joyce, G., & Yokoyama, T. (2010). Density enhancements associated with equatorial spread *F*. *Annales Geophysicae*, *28*(2), 327–337. <https://doi.org/10.5194/angeo-28-327-2010>
- Krall, J., Huba, J. D., Ossakow, S. L., & Joyce, G. (2010). Equatorial spread *F* fossil plumes. *Annales Geophysicae*, *28*(11), 2059–2069. <https://doi.org/10.5194/angeo-28-2059-2010>
- Le, G., Huang, C.-S., Pfaff, R. F., Su, S.-Y., Yeh, H.-C., Heelis, R. A., et al. (2003). Plasma density enhancements associated with equatorial spread *F*: ROCSAT-1 and DMSP observations. *Journal of Geophysical Research*, *108*(A8), 1318. <https://doi.org/10.1029/2002JA009592>
- Makela, J., & Otsuka, Y. (2011). Overview of nighttime ionospheric instabilities at low- and mid-latitudes: Coupling aspects resulting in structuring at the mesoscale. *Space Science Reviews*, *168*(1-4), 419–440. <https://doi.org/10.1007/s11214-011-9816-6>

- Martinis, C., Baumgardner, J., Mendillo, M., Su, S.-Y., & Aponte, N. (2009). Brightening of 630.0 nm equatorial spread-F airglow depletions. *Journal of Geophysical Research*, *114*, A06318. <https://doi.org/10.1029/2008JA013931>
- Martinis, C., Baumgardner, J., Wroten, J., & Mendillo, M. (2011). All-sky imaging observations of conjugate medium-scale traveling ionospheric disturbances in the American sector. *Journal of Geophysical Research*, *116*, A05326. <https://doi.org/10.1029/2010JA016264>
- Miller, E. S., Kil, H., Makela, J. J., Heelis, R. A., Talaat, E. R., & Gross, A. (2014). Topside signature of medium-scale traveling ionospheric disturbances. *Annales Geophysicae*, *32*(8), 959–965. <https://doi.org/10.5194/angeo-32-959-2014>
- Otsuka, Y., Shiokawa, K., Ogawa, T., & Wilkinson, P. (2004). Geomagnetic conjugate observations of medium-scale traveling ionospheric disturbances at midlatitude using all-sky airglow imagers. *Geophysical Research Letters*, *31*, L15803. <https://doi.org/10.1029/2004GL020262>
- Otsuka, Y., Shiokawa, K., Ogawa, T., Yokoyama, T., & Yamamoto, M. (2009). Spatial relationship of nighttime medium-scale traveling ionospheric disturbances and F region field-aligned irregularities observed with two spaced all-sky airglow imagers and the middle and upper atmosphere radar. *Journal of Geophysical Research*, *114*, A05302. <https://doi.org/10.1029/2008JA013902>
- Park, J., Min, K. W., Kim, V. P., Kil, H., Kim, H. J., Lee, J. J., et al. (2008). Statistical description of low-latitude plasma blobs as observed by DMSP F15 and KOMPSAT-1. *Advances in Space Research*, *41*(4), 650–654. <https://doi.org/10.1016/j.asr.2007.04.089>
- Park, J., Min, K. W., Lee, J.-J., Kil, H., Kim, V. P., Kim, H.-J., et al. (2003). Plasma blob events observed by KOMPSAT-1 and DMSP F15 in the low latitude nighttime upper ionosphere. *Geophysical Research Letters*, *30*(21), 2114. <https://doi.org/10.1029/2003GL018249>
- Prölss, G. W. (1995). In H. Volland (Ed.), *Ionospheric F region storms: Handbook of Atmospheric Electrodynamics* (Vol. 2, pp. 195–248). Boca Raton: CRC Press.
- Saito, A., Nishimura, M., Yamamoto, M., Fukao, S., Kubota, M., Shiokawa, K., et al. (2001). Traveling ionospheric disturbances detected in the FRONT campaign. *Geophysical Research Letters*, *28*(4), 689–692. <https://doi.org/10.1029/2000GL011884>
- Shiokawa, K., Ihara, C., Otsuka, Y., & Ogawa, T. (2003). Statistical study of nighttime medium-scale traveling ionospheric disturbances using midlatitude airglow images. *Journal of Geophysical Research*, *108*(A1), 1052. <https://doi.org/10.1029/2002JA009491>
- Yokoyama, T., Su, S.-Y., & Fukao, S. (2007). Plasma blobs and irregularities concurrently observed by ROCSAT-1 and Equatorial Atmosphere Radar. *Journal of Geophysical Research*, *112*, A05311. <https://doi.org/10.1029/2006JA012044>